

1
2
3
4 1 **$\delta^{18}\text{O}$ and $\delta^{13}\text{C}$ of *Cyprideis torosa* from coastal lakes: modern systematics and down-**
5 2 **core interpretation**

6 3 Roberts, L.R.^{1,2,a}, Holmes, J.A.^{2*}, Sloane, H.J.³, Arrowsmith, C.³, Leng, M.J.^{3,4} and Horne, D.J.¹
7
8 4

9 5 ¹*School of Geography, Queen Mary University of London, Mile End Road, London, E1 4NS,*
10 6 *UK*

11 7 ²*Environmental Change Research Centre, Department of Geography, University College*
12 8 *London, Gower Street, London, WC1E 6BT, UK*

13 9 ³*National Environmental Isotope Facility, British Geological Survey, Keyworth, Nottingham,*
14 10 *NG12 5GG, UK*

15 11 ⁴*Centre for Environmental Geochemistry, School of Biosciences, University of Nottingham,*
16 12 *Sutton Bonington Campus, Loughborough LE12 5RD, UK*

17 13
18 14 ^a*Current address: Centre for Environmental Geochemistry, School of Geography, University*
19 15 *of Nottingham, Nottingham, NG7 2RD, UK*
20 16

21 17 *j.holmes@ucl.ac.uk
22 18
23 19

24 20 **Abstract**
25 21

26 22 Stable isotope analyses of ostracod shells are a commonly-used proxy for
27 23 palaeoenvironmental reconstruction. Although the fundamental controls on isotope
28 24 composition of ostracod shells are well understood and, in some instances, quantifiable, the
29 25 paleoclimatic and palaeoenvironmental interpretation of records from lake sediments depends
30 26 strongly on the characteristics of individual lakes including the climatic setting, depth, volume,
31 27 hydrology, aquatic vegetation and catchment properties. This is particularly important for
32 28 coastal lakes where physio-chemical variations may occur on diurnal timescales. Here, we
33 29 combine variations in $\delta^{18}\text{O}_{\text{water}}$, $\delta^{18}\text{O}_{\text{ostracod}}$ and $\delta^{13}\text{C}_{\text{ostracod}}$, hourly water temperature, and
34 30 $\text{Mg}/\text{Ca}_{\text{ostracod}}$ inferred water temperatures (constraining calcification temperature) to improve
35 31 palaeoenvironmental interpretation and provide insights into lake carbon cycle. The dataset
36 32 improves understanding of complex coastal lake site systematics and downcore interpretation
37 33 of stable isotopes from *C. torosa*, a geographically widespread brackish water ostracod. The
38 34 $\delta^{18}\text{O}_{\text{ostracod}}$ values show a complex relationship with temperature and suggest, in most
39 35 circumstances, that $\delta^{18}\text{O}_{\text{water}}$ is the dominant control on $\delta^{18}\text{O}_{\text{ostracod}}$. During times of fresher
40 36 water, $\delta^{13}\text{C}_{\text{ostracod}}$ increases, suggesting increasing aquatic productivity. Above a certain
41 37 $\delta^{18}\text{O}_{\text{water}}$ threshold however, aquatic productivity begins to decline. The interpretation of
42 38 $\delta^{13}\text{C}_{\text{ostracod}}$ in some coastal lakes, may therefore be dependent on understanding of the range
43 39 of expected $\delta^{18}\text{O}_{\text{water}}$. Due to short-term (diurnal to seasonal) variations that cause large
44
45
46
47
48
49
50
51
52
53
54
55
56
57
58
59
60

61
62
63 40 ranges in $\delta^{18}\text{O}_{\text{water}}$ and $\delta^{18}\text{O}_{\text{ostracod}}$, stable isotope analyses of *C. torosa* should be: 1)
64 41 undertaken on multiple single shells 2) where carapaces are preserved, paired with trace-
65 42 element/Ca analyses on the same individual; and 3) undertaken alongside a study of the
66 43 modern lake system.
67
68
69
70

71 45 **Keywords:** *Cyprideis torosa*; ostracods; stable isotopes; oxygen isotope; carbon isotope;
72 46 coastal lakes; palaeoenvironmental reconstruction
73

74 47 75 48 76 49 **1. Introduction**

77 50 Inorganic and biogenic carbonates precipitated from lake water provide an archive of past
78 51 oxygen ($\delta^{18}\text{O}$) and carbon ($\delta^{13}\text{C}$) isotope composition of host water and dissolved inorganic
79 52 carbon (DIC), and, for oxygen, potentially water temperature as well. For palaeoenvironmental
80 53 studies, there are advantages in analysing biogenic over endogenic carbonate. For example,
81 54 the use of biogenic carbonate can reflect taphonomic or habitat-specific stable isotope
82 55 composition while the use of endogenic carbonate does not guarantee that the material was
83 56 formed in water and may include a detrital component. The calcite shells of ostracods (small
84 57 bivalved crustaceans) are often abundant and well preserved in sediments, providing a
85 58 commonly used proxy for palaeoenvironmental studies. The calcification of carapaces occurs
86 59 within hours to a few days with no subsequent addition of calcite, thus providing a 'snapshot'
87 60 of water conditions at the timing of calcification. This is very different to the 'averaging' of
88 61 conditions recorded by endogenic carbonate and other types of biogenic carbonates that
89 62 accumulate incrementally. Where the life cycle and habitat preferences of a species is known,
90 63 isotopic records may therefore reflect seasonal and habitat-specific information (e.g. von
91 64 Grafenstein *et al.*, 1999a).
92
93
94
95
96
97
98
99

100 65 The oxygen-isotope composition of biogenic and endogenic calcite is determined by water
101 66 temperature and water-isotope composition, along with any kinetic vital effects. During growth,
102 67 the carbonate ions (CO_3^{2-}) are generally thought to be in equilibrium with the isotope
103 68 composition of the water. However, since CO_3^{2-} ions are precipitated together with calcium to
104 69 form calcium carbonate, heavy isotopes are preferentially incorporated (Kim and O'Neil, 1997;
105 70 Romanek *et al.*, 1992). Substantial evidence exists to suggest that ostracod calcite is
106 71 precipitated out of oxygen isotope equilibrium with the host water, by +3 ‰ or more (Xia *et al.*,
107 72 1997; von Grafenstein *et al.*, 1999b; Chivas *et al.*, 2002; Keatings *et al.*, 2002; Decrouy *et al.*,
108 73 2011). The magnitude of offset appears to vary taxonomically; vital offsets are similar for
109 74 members of the same genus, or even subfamily.
110
111
112
113
114
115
116
117
118
119
120

121
122
123 76 Since the $\delta^{18}\text{O}_{\text{calcite}}$ is a function of temperature and $\delta^{18}\text{O}_{\text{water}}$, if the calcification temperature
124
125 77 is known independently, the $\delta^{18}\text{O}_{\text{water}}$ can be calculated, for example using the equation of Kim
126 78 and O'Neil (1997), $1000\ln\alpha_{(\text{calcite-water})} = 18.03(10^3T^{-1}) - 32.42$. However, the equation relies on
127 79 the assumption that mineral precipitation is controlled by $\delta^{18}\text{O}_{\text{water}}$ at the time of calcification
128 80 and that any vital effects are known and accounted for (von Grafenstein *et al.*, 1999b).
129 81 $\delta^{18}\text{O}_{\text{water}}$ is a function of $\delta^{18}\text{O}$ rainfall, $\delta^{18}\text{O}$ of catchment inputs, evaporative enrichment or a
130 82 combination of all three. $\delta^{18}\text{O}_{\text{ostracod}}$ has, therefore, been used to reconstruct: the composition
131 83 of rainfall (von Grafenstein, 2002), effective moisture (Hodell *et al.*, 1991; Street-Perrott *et al.*,
132 84 2000; Holmes *et al.*, 2010), meltwater influx (Dettman *et al.*, 1995), and changes in seawater
133 85 input (Janz and Vennemann, 2005; Williams *et al.*, 2006).
134
135
136
137
138 86

139 87 The $\delta^{13}\text{C}$ of ostracod shells is primarily determined by the $\delta^{13}\text{C}$ of DIC with only a small
140 88 temperature effect during calcite precipitation (Leng and Marshall, 2004). Offsets from carbon-
141 89 isotope equilibrium appear to be negligible although, at present, there is limited understanding
142 90 of carbon isotope fractionation in ostracod shells. Since many ostracod species are not
143 91 nektonic (including *Cyprideis torosa*), the $\delta^{13}\text{C}$ often does not reflect open water conditions,
144 92 but more localised dissolved inorganic carbon (DIC) of pore water or water at the sediment
145 93 interface, which is often more strongly correlated with the breakdown of sediment organic
146 94 matter than primarily productivity. However, in very shallow well-mixed waterbodies with few
147 95 submerged macrophytes, there may be little difference in DIC composition between the
148 96 ambient water in the water column and the sediment-water interface. Furthermore, it is still
149 97 unknown if ostracod species calcify in the sediment or in the water column. Despite this,
150 98 Wrozyña *et al.* (2012) showed that with increasing productivity, plankton preferentially uptake
151 99 ^{12}C and the remaining DIC is enriched with ^{13}C , which is consequently incorporated into
152 100 carbonates. As a result of decay of organic matter, ambient water is enriched in ^{12}C and
153 101 ostracods are consequently depleted in ^{13}C so that $\delta^{13}\text{C}$ values are more negative. Differences
154 102 in species $\delta^{13}\text{C}$ values are therefore often regarded as habitat effects rather than true vital
155 103 effects (Heaton *et al.* 1995). Given this, ostracod-based $\delta^{13}\text{C}$ are not straight forward to
156 104 interpret, but they have been used to reconstruct aquatic productivity (Anadón *et al.*, 2006; Li
157 105 and Liu, 2014) and provide evidence for methane formation (Bridgwater *et al.*, 1999).
158
159
160
161
162
163
164
165
166
167 106

168 107 Although the fundamental controls on isotope composition of ostracod shells are well
169 108 understood and, in some instances, quantifiable, the paleoclimatic and palaeoenvironmental
170 109 interpretation of isotope records from lake sediments depends strongly on the characteristics
171 110 of individual lakes including the climatic setting, depth, volume, hydrology, aquatic vegetation
172 111 and catchment properties. These are particularly important considerations for coastal lakes,
173 112 ponds, and lagoons where complex diurnal mixing of water masses often results in changes
174
175
176
177
178
179
180

181
182
183
184
185
186
187
188
189
190
191
192
193
194
195
196
197
198
199
200
201
202
203
204
205
206
207
208
209
210
211
212
213
214
215
216
217
218
219
220
221
222
223
224
225
226
227
228
229
230
231
232
233
234
235
236
237
238
239
240

113 to solute chemistry, water depth, and, in some cases, temperature. Marginal-marine
114 environments including estuaries, deltas and coastal lakes/ponds with both direct and indirect
115 seawater connection are complex, unstable, and often unpredictable environments due to the
116 variation in physio-chemical conditions from the complex mixing of fresh- and sea- water.
117 These variations are due to climatic (precipitation/evaporation cycles) and dynamic (tides,
118 currents, freshwater drainage and sea level changes) factors (Carbonel, 1988; Dix *et al.*,
119 1999). The mixing of freshwater and seawater results in a theoretical straight mixing line of
120 $\delta^{18}\text{O}$. However, Anadón *et al.* (2002) suggest that the natural variations in this relationship,
121 often resulting from a third end member such as groundwater, prohibits the use of $\delta^{18}\text{O}_{\text{ostracod}}$
122 as a palaeotemperature proxy unless paired with Mg/Ca-inferred temperatures (e.g. Ingram
123 *et al.* 1998). An understanding of the modern isotope systematics of the site, and the life-cycle
124 and habitat preferences of the target ostracod species are therefore important constraints
125 when interpreting isotopic signatures (Decrouy *et al.*, 2011).

126
127 The robust well-calcified carapace of *Cyprideis torosa* is a valuable source of Quaternary
128 paleoclimatic information. It is geographically widespread (Wouters, 2017) and tolerant of a
129 wide range of ecological conditions. Most notably, it is extremely euryhaline, and found in
130 waters from fresh to hypersaline (De Deckker and Lord, 2017; Pint and Frenzel, 2017; Scharf
131 *et al.*, 2017) although in saline waters it is restricted to those with a marine-like chemistry.
132 Furthermore there is a good understanding of the adult life-cycle (e.g. Heip, 1976) and there
133 are existing Mg/Ca palaeotemperature calibrations (e.g. Wansard 1996; De Deckker *et al.*
134 1999).

135
136 Due to temperature and $\delta^{18}\text{O}_{\text{water}}$ varying on short (diurnal) timescales in coastal lakes, water
137 conditions at the time of ostracod sample collection can be substantially different to those at
138 the time of shell calcification. As such, establishing the temperature and $\delta^{18}\text{O}_{\text{water}}$ at the exact
139 time of shell calcification for *C. torosa* is difficult (Marco-Barba *et al.*, 2012; Bodergat *et al.*
140 2014). There are therefore two large uncertainties when interpreting *C. torosa* stable isotope
141 records from coastal lakes; 1) what the dominant controls are on $\delta^{18}\text{O}_{\text{ostracod}}$, and 2) whether
142 short-term (seasonal) lake variations are recorded in sediment records. There are often large
143 uncertainties in the interpretation of stable isotope signals from *C. torosa*, in part arising from
144 the paucity of studies into the impact of the diurnal and seasonal variations in coastal lakes
145 on the isotope geochemistry of ostracod shells. Here, we investigate how the isotope
146 systematics of a coastal pond are recorded in shells of *C. torosa* using a dataset of water
147 isotopes, water chemistry and ostracod isotopes in order to improve the interpretation of
148 ostracod stable isotope signals from sediment records. We combine measurements of
149 $\delta^{18}\text{O}_{\text{ostracod}}$ with Mg/Ca_{ostracod}-inferred water temperatures to back calculate $\delta^{18}\text{O}_{\text{water}}$, and



241
242
243
244
245
246
247
248
249
250
251
252
253
254
255
256
257
258
259
260
261
262
263
264
265
266
267
268
269
270
271
272
273
274
275
276
277
278
279
280
281
282
283
284
285
286
287
288
289
290
291
292
293
294
295
296
297
298
299
300

150 evaluate these using measurements of seasonal and diurnal water temperature and of water-
151 isotope composition. A more limited set of carbon-isotope data is used to investigate seasonal
152 changes in carbon-cycling within the lake. Understanding the nature of these variations and
153 their controls has important implications for the interpretation of fossil records from similar
154 environments. The results presented here follow a previous study using the $Mg/Ca_{ostracod}$ of
155 the same specimens to track the seasonal calcification of individuals within a population
156 (Roberts *et al.*, 2020).

157

158 **2. Methods**

159

160 **2.1 Field methods**

161

162 Material for this study collected from a shallow (< 1 m) coastal pond free from submerged and
163 floating macrophytes in Pegwell Bay Nature Reserve, Kent, SE UK (Fig. 1), where *C. torosa*
164 is particularly abundant, in August and December 2016 and April, June and September 2017.
165 Ostracods were collected in a 250 μm zooplankton net from the top 1 cm of sediment at
166 location 'X' (Fig. 1). Adult carapaces with soft tissue and appendages (indicating that the
167 individuals were alive at the time of collection) were selected for geochemical analyses. Water
168 samples for oxygen and hydrogen isotope composition were collected as spot samples for all
169 dates except June 2017 when samples were collected hourly from low to high tide to capture
170 diurnal hydro-chemical variability. A seawater end-member sample was collected adjacent to
171 Ramsgate Harbour in April 2017. In situ measurements of conductivity and temperature were
172 taken using a YSI 30 handheld probe calibrated and recorded at 25 °C. Hourly subsurface (~
173 10cm) water temperature was recorded from August 2016 to September 2017 using a Tinytag
174 Aquatic 2 temperature logger with temperature range -40 °C to +70 °C. For the April and June
175 2017 sampling, in situ alkalinity as $CaCO_3$ equivalent was determined using a Hach Digital
176 Titrator, 1.6N Sulphuric acid (H_2SO_4) cartridge and Phenolphthalein and Bromcresol Green-
177 Methyl Red indicators.

178

179 **2.2 Laboratory methods**

180

181 Stable isotope analysis was undertaken on single left valves using an IsoPrime dual inlet mass
182 spectrometer plus Multiprep at the British Geological Survey. Isotope values ($\delta^{13}C$, $\delta^{18}O$) are
183 reported as per mille (‰) deviations of the isotope ratios ($^{13}C/^{12}C$, $^{18}O/^{16}O$) calculated to the
184 VPDB scale using a within-run laboratory standard calibrated against NBS-19. The Craig
185 correction was applied to account for ^{17}O . Analysis of the in-house standard calcite (KCM)

301
302
303 186 gave good reproducibility of ± 0.04 for both $\delta^{13}\text{C}$ and $\delta^{18}\text{O}$ over 72 determinations. Mg/Ca and
304 187 Sr/Ca determinations were undertaken on the corresponding right valves of the same
305 188 individuals used for stable isotope analyses, as described in Roberts *et al.* (2020).
306
307
308

309 190 $\delta^{18}\text{O}$ analyses of water were undertaken using the CO_2 equilibration method on an IsoPrime
310 191 100 mass spectrometer plus Aquaprep at the British Geological Survey. Hydrogen isotope
311 192 ($\delta^2\text{H}$) measurements of water were made using an online Cr reduction method with a
312 193 EuroPyrOH-3110 system coupled to a IsoPrime mass spectrometer. Values are reported as
313 194 per mille (‰) deviations of the isotope ratios ($^{18}\text{O}/^{16}\text{O}$ and $^2\text{H}/^1\text{H}$) calculated to the VSMOW
314 195 scale. Internal quality control standards are calibrated against the international standards
315 196 VSMOW2 and VSLAP2 with average errors of ± 0.05 ‰ for $\delta^{18}\text{O}$ and ± 1.0 ‰ for $\delta^2\text{H}$.
316
317
318
319
320

321 198 **2.3 Calculations**

322 199
323
324 200 If the $\delta^{18}\text{O}_{\text{calcite}}$ and water temperature at the time of calcite precipitation are known, the
325 201 expected $\delta^{18}\text{O}_{\text{water}}$ value can be calculated using one of several empirical equations. However,
326 202 because ostracod shells do not calcify in oxygen-isotope equilibrium with their host water,
327 203 corrections must be made for vital offsets. For *Cyprideis torosa*, the best estimate for the vital
328 204 offset is $\sim +0.8$ ‰ (Keatings *et al.*, 2007).
329
330
331

332 206 The water temperature at the time of calcification can be determined using the Mg content for
333 207 the corresponding valve to that used for isotope analysis, and the equation of De Deckker *et*
334 208 *al.* (1999):
335
336
337

$$338 \quad T(^{\circ}\text{C}) = 2.69 + (5230 * [\text{Mg}/\text{Ca}]_{\text{ostracod}} / [\text{Mg}/\text{Ca}]_{\text{water}}) \quad (1)$$

340 211
341 212
342 213 A $\text{Mg}/\text{Ca}_{\text{water}}$ of 4.2 mol/mol (the average measured $\text{Mg}/\text{Ca}_{\text{water}}$ value; Roberts *et al.*, 2020) is
343 214 used in the equation.
344
345
346

347 216 The Mg/Ca-inferred temperatures are combined with $\delta^{18}\text{O}_{\text{ostracod}}$ values to determine $\delta^{18}\text{O}_{\text{water}}$
348 217 using Kim and O'Neil (1997):
349
350

$$351 \quad 1000 \ln \alpha_{(\text{calcite-water})} = 18.03(10^3 T^{-1}) - 32.42 \quad (2)$$

352 219
353 220 Where T is in kelvins.
354
355
356
357
358
359
360

361
362
363
364
365
366
367
368
369
370
371
372
373
374
375
376
377
378
379
380
381
382
383
384
385
386
387
388
389
390
391
392
393
394
395
396
397
398
399
400
401
402
403
404
405
406
407
408
409
410
411
412
413
414
415
416
417
418
419
420

223 The fractionation factor ($\alpha_{\text{calcite-water}}$) can be calculated using:

224
225
$$\alpha_{\text{calcite-water}} = (1000 + \delta^{18}\text{O}_{\text{calcite}}) / (1000 + \delta^{18}\text{O}_{\text{water}})$$

226 (3)

227
228 Where both $\delta^{18}\text{O}_{\text{calcite}}$ and $\delta^{18}\text{O}_{\text{water}}$ are expressed relative to VSMOW. To convert from VPDB
229 to VSMOW, the conversion proposed by Coplen *et al.* (1983) was used:

230
231
$$\delta^{18}\text{O}_{\text{VSMOW}} = 1.03091 * \delta^{18}\text{O}_{\text{VPDB}} + 30.91$$

232 (4)

234 3. Results

236 3.1 Water isotope composition

237
238 $\delta^{18}\text{O}_{\text{water}}$ values measured throughout the year ranged from -2.84 to $+4.85$ ‰. Highest $\delta^{18}\text{O}$
239 values were recorded in August ($+3.86$ ‰) and June ($+4.85$ ‰) (Table 1; Fig. 2a). Water
240 sampled in December to April had lower $\delta^{18}\text{O}$ values, with the lowest value of -2.84 ‰
241 recorded in December. There is a strong relationship ($R^2 = 0.86$) between $\delta^{18}\text{O}_{\text{water}}$ and
242 electrical conductivity (EC) (Fig. 3): this relationship is particularly pronounced for the values
243 recorded in June when the highest $\delta^{18}\text{O}_{\text{water}}$ values ($+4.85$ ‰) and EC values (75.2 mS cm^{-1})
244 are recorded (Fig. 2b). There is a strong distinction between the summer samples (June and
245 August) and samples taken in September to April; the summer months are characterised by
246 high $\delta^{18}\text{O}$ values. Water temperature and $\delta^{18}\text{O}_{\text{water}}$ display similar trends with increasing values
247 between December 2016 and June 2017 (Fig. 2c) In September, the $\delta^{18}\text{O}_{\text{water}}$ was close to the
248 seawater equivalent (-0.06 ‰ in the pond, and $+0.27$ ‰ adjacent to Ramsgate Harbour) (Fig.
249 4) and reflects a drop in EC (Fig. 2a,b). Spatially there is little variation in isotope composition
250 of pond water (Table 2); $\delta^2\text{H}$ and $\delta^{18}\text{O}$ were slightly lower at location 5 and 6 compared to the
251 southern end of the pond.

253 3.2 Ostracod shell chemistry

254
255 $\delta^{18}\text{O}_{\text{ostracod}}$ values also suggest a seasonal pattern; valves collected in April, June and
256 September 2017 have lower $\delta^{18}\text{O}$ (with a mean value -6.10 ‰) and those from December
257 2016 and February 2017 are higher (a mean value of $+1.80$ ‰) (Fig 2d; Table 3). All $\delta^{18}\text{O}_{\text{ostracod}}$
258 values for April, June, and September 2017 are negative (minimum value of -11.38 ‰), but

421
422
423 259 the mean $\delta^{18}\text{O}_{\text{ostracod}}$ value for August 2016 is +1.24 ‰. For the August 2016, December 2016,
424
425 260 and February 2017 collections, the range of values is similar for all months (± 3.8 ‰, 5.0 ‰,
426
427 261 and 4.3 ‰ respectively). For samples collected in April and September 2017 the range is
428
429 262 smaller at 2.6 and 2.9 ‰. The largest range is 7.2 ‰ for samples collected in June 2017.
430
431 263 $\text{Mg}/\text{Ca}_{\text{ostracod}}$ is also strongly seasonal with gradually decreasing values recorded in April to
432
433 264 September with the lowest average values in December and February (7.88 and 8.24
434
435 265 mmol/mol) (Fig. 2e; Table 3). The range of values is highest in August 2016 (± 22.09 mmol/mol)
436
437 266 and June 2017 (± 22.45 mmol/mol) (Fig. 2e).

436 267 If the seasonal variation in $\delta^{18}\text{O}_{\text{ostracod}}$ were being controlled primarily by water temperature,
437
438 268 a negative relationship between $\text{Mg}/\text{Ca}_{\text{ostracod}}$ and $\delta^{18}\text{O}_{\text{ostracod}}$ would be expected. However,
439
440 269 such a relationship is not seen in this dataset as a whole, although there is a negative
441
442 270 relationship for the samples taken in August 2016, December 2016 and February 2017 (Fig.
443
444 271 5a). The majority of samples from April, June and September 2017 do not follow the
445
446 272 relationship defined by Kim and O'Neil (1997). There is also a distinct separation of the
447
448 273 relationship between $\delta^{18}\text{O}_{\text{ostracod}}$ and $\text{Sr}/\text{Ca}_{\text{ostracod}}$ for samples collected in April, June and
449
450 274 September 2017 from samples collected in August 2016, December 2016 and February 2017
451
452 275 (Fig. 5b); the former have $\delta^{18}\text{O}_{\text{ostracod}}$ values equivalent to freshwater (mean of -6.14 ‰) while
453
454 276 the latter are characterised by high $\delta^{18}\text{O}_{\text{ostracod}}$ values (mean of $+1.62$ ‰). Unlike $\delta^{18}\text{O}_{\text{ostracod}}$
455
456 277 and $\text{Mg}/\text{Ca}_{\text{ostracod}}$, $\text{Sr}/\text{Ca}_{\text{ostracod}}$ is similar throughout the year (± 2.19 mmol/mol) with the highest
457
458 278 value in June 2017 (4.23 mmol/mol) and lowest in August (2.04 mmol/mol) (Fig. 5b).

459
460 279
461
462 280 $\delta^{13}\text{C}_{\text{ostracod}}$ values mirror those of $\delta^{18}\text{O}_{\text{ostracod}}$, with higher values in April 2017, June 2017, and
463
464 281 September 2017 when $\delta^{18}\text{O}_{\text{ostracod}}$ values are lower (Fig. 2f). The $\delta^{13}\text{C}$ values for August 2016
465
466 282 are unlike those observed for Summer in 2017; the average $\delta^{13}\text{C}$ value for August 2016 is $-$
467
468 283 5.69 ‰ compared with -0.59 ‰ in June 2017 and $+0.93$ ‰ in September 2017. The value of
469
470 284 -5.69 ‰ is similar to those recorded in December (-6.16 ‰) and February 2016 (-6.16 ‰)
471
472 285 when $\delta^{18}\text{O}_{\text{ostracod}}$ values are higher. Furthermore, in April, June, and September 2017 there is
473
474 286 a positive relationship between $\delta^{18}\text{O}_{\text{ostracod}}$ and $\delta^{13}\text{C}_{\text{ostracod}}$ while the August 2016, December
475
476 287 2016, and February 2017 samples have a negative relationship (Fig. 5c). Whilst the samples
477
478 288 from April, June and September 2017 have a distinct separate clustering in terms of isotopic
479
480 289 composition, this is not reflected in the Mg/Ca and Sr/Ca values with no relationship seen
481
482 290 across the dataset (Fig. 5d).

471 291 472 292 **3.3 Back calculated $\delta^{18}\text{O}_{\text{water}}$** 473 293

481
482
483
484
485
486
487
488
489
490
491
492
493
494
495
496
497
498
499
500
501
502
503
504
505
506
507
508
509
510
511
512
513
514
515
516
517
518
519
520
521
522
523
524
525
526
527
528
529
530
531
532
533
534
535
536
537
538
539
540

294 Back calculated $\delta^{18}\text{O}_{\text{water}}$ values range from +5.37 to -7.65 ‰ (Table 3). For the two
295 populations identified above (1 – individuals collected in August 2016, December 2016, and
296 February 2017 and 2 – individuals collected in April, June, and September 2017), the back
297 calculated values for August 2016, December 2016, and February 2017 are 5.37 to -1.86 ‰
298 and 1.80 to -7.65 ‰ for April, June, and September 2017.

4. Discussion

302 In the pond at Pegwell Bay, the dominant controls on $\delta^{18}\text{O}_{\text{ostracod}}$ are $\delta^{18}\text{O}_{\text{water}}$ (influenced by
303 input cycles of seawater and meteoric water) and temperature. Due to the shallow, well-mixed,
304 and habitat homogeneity of the Pegwell Bay pond, it is reasonable to assume that the
305 dominant control on $\delta^{13}\text{C}_{\text{ostracod}}$ is the breakdown of organic matter in the near surface
306 sediments from increasing terrestrial and aquatic productivity. For trace-element/ $\text{Ca}_{\text{ostracod}}$ the
307 dominant controls in the Pegwell Bay pond are temperature for $\text{Mg}/\text{Ca}_{\text{ostracod}}$ and $\text{Sr}/\text{Ca}_{\text{water}}$ for
308 $\text{Sr}/\text{Ca}_{\text{water}}$ (see Roberts *et al.*, 2020).

310 In a biplot of water $\delta^{18}\text{O}$ and $\delta^2\text{H}$, the values for Pegwell lie on a lower gradient to the global
311 meteoric water line (GMWL) (Fig. 4), demonstrating evaporative loss along the local
312 evaporative line (LEL), with the seawater end member falling close to the LEL. Seasonal
313 samples further confirm that evaporation is predominately driving salinity in the pond with high
314 EC and elevated $\delta^{18}\text{O}$ values recorded in months with high water temperature and vice versa
315 (August and December respectively; Table 1, Table 4). Evaporation therefore appears to be
316 seasonal and to be particularly pronounced in the warmer months, with $\delta^{18}\text{O}_{\text{water}}$ values
317 reaching +4.85 ‰ in June 2017 (the pond also dried out in 2009; Google Maps Street View,
318 2018). Samples from April with similar $\delta^{18}\text{O}$ values to the seawater $\delta^{18}\text{O}$ end member suggest
319 that on occasion there was a direct input of seawater, which may occur at extreme tidal events
320 such as the spring equinox tide. Furthermore, the $\text{Mg}/\text{Ca}_{\text{water}}$ and $\text{Sr}/\text{Ca}_{\text{water}}$ values of 4.14
321 mol/mol and 0.010 mol/mol are similar to seawater, although Mg/Ca is slightly lower than that
322 of average seawater (5.1 mol/mol) suggesting some dilution, while the Sr/Ca is slightly higher
323 than that of average seawater (0.0089 mol/mol) (Chester, 2000). In summary, therefore,
324 seawater input and evaporation appear to be a primary controls on $\delta^{18}\text{O}_{\text{ostracod}}$ with summer
325 samples reflecting high temperatures and high $\delta^{18}\text{O}_{\text{water}}$ and autumn/winter samples to reflect
326 lower temperatures, higher precipitation, and therefore lower $\delta^{18}\text{O}_{\text{water}}$.

328 On PCA biplots of environmental variables for each collection, $\delta^{18}\text{O}_{\text{water}}$ explains 79.28 % of
329 the variance (Fig. 6). August, June, and September 2017 are characterised by higher
330 temperature, with June and August also having higher EC and $\delta^{18}\text{O}_{\text{water}}$. Autumn/winter waters

541
542
543
544
545
546
547
548
549
550
551
552
553
554
555
556
557
558
559
560
561
562
563
564
565
566
567
568
569
570
571
572
573
574
575
576
577
578
579
580
581
582
583
584
585
586
587
588
589
590
591
592
593
594
595
596
597
598
599
600

331 (i.e. October to November) are characterised by low temperature and low $\delta^{18}\text{O}_{\text{water}}$. However,
332 the September $\delta^{18}\text{O}_{\text{ostracod}}$ values show a discrete clustering (Fig. 5a) that may relate to the
333 lower electrical conductivity and $\delta^{18}\text{O}_{\text{water}}$ values in this month compared to others (Table 1).
334 Furthermore, September back-calculated $\delta^{18}\text{O}_{\text{water}}$ values are as low as -7.65‰ (equivalent
335 to the isotopic composition of rainfall for SE England: Darling et al., 2003), suggesting that
336 valves calcified in waters with a much greater input of meteoric water. Using the Mg/Ca-
337 inferred temperature and monitored water temperatures to track the calcification months of
338 collected valves, the September 2017 collection reflects conditions between April and July
339 2017. June and July 2017 received high rainfall (74.2 and 85.6 mm respectively compared
340 with a mean of 42.7 and 47.6 mm between 1934 and 2016; Table 4). The monitored waters
341 (-1.19‰ for April 2017 and $+4.85\text{‰}$ for June 2017), however, suggest a considerable degree
342 of evaporative enrichment and/or significant seawater input, which is plausible given the high
343 temperatures (Table 1) and our basic understanding of site systematics. If the monitored
344 $\delta^{18}\text{O}_{\text{water}}$ values are considered when interpreting the dataset, it would appear that the pond is
345 highly evaporated, however, it is clear that pond water was equivalent to groundwater or local
346 precipitation during June and July. The composition of the pond can therefore shift quickly (on
347 a less than monthly timescale).

348
349 The $\delta^{18}\text{O}_{\text{ostracod}}$ values show a complex relationship with temperature. The individual $\delta^{18}\text{O}_{\text{ostracod}}$
350 values for collection in August 2016, December 2016 and February 2017 show some scatter,
351 but follow the relationship between water temperature and calcite oxygen-isotope values
352 based on the equation of Kim and O'Neil (1997) (Fig. 5a). However, $\delta^{18}\text{O}_{\text{ostracod}}$ values for
353 collections in April, June and September 2017 do not follow this relationship, suggesting that
354 $\delta^{18}\text{O}_{\text{water}}$ is a more important control on $\delta^{18}\text{O}_{\text{ostracod}}$. Despite this, $\text{Mg}/\text{Ca}_{\text{ostracod}}$, $\text{Sr}/\text{Ca}_{\text{ostracod}}$,
355 temperatures and monitored $\delta^{18}\text{O}_{\text{water}}$ values are not distinctly different than in August 2016,
356 December 2016 and February 2017. The primary hydrological difference is that in July and
357 August 2016 there was lower precipitation than the same period in 2017 (10.8 and 18.0 mm
358 respectively; Met Office 2012), which is reflected in the back calculated $\delta^{18}\text{O}_{\text{water}}$ values (mean
359 values of $+2.17\text{‰}$ for valves collected in August 2016 compared with -4.75‰ for September
360 2017), suggesting that $\delta^{18}\text{O}_{\text{water}}$ becomes the primary control on $\delta^{18}\text{O}_{\text{ostracod}}$ during periods of
361 lower $\delta^{18}\text{O}_{\text{water}}$.

362
363 Changes in $\delta^{18}\text{O}$ and $\delta^{13}\text{C}$ in individual shells and in the different sampling periods provides
364 insight into the influences on carbon-isotope signatures at Pegwell. Shells with lower $\delta^{18}\text{O}$
365 have higher $\delta^{13}\text{C}_{\text{ostracod}}$, suggesting that a greater amount of freshwater in the pond
366 accompanies an increase in aquatic productivity, assuming that $\delta^{13}\text{C}_{\text{DIC}}$ is a first-order proxy
367 for aquatic productivity. Shells with higher $\delta^{18}\text{O}$ have lower $\delta^{13}\text{C}_{\text{ostracod}}$, suggesting that elevated

601
602
603 368 evaporation or input of seawater is accompanied by oxidation of terrestrially-derived organic
604 matter. This shift in relationship of positive carbon-oxygen covariance at lower $\delta^{18}\text{O}_{\text{water}}$ to
605 369 negative at higher $\delta^{18}\text{O}_{\text{water}}$ (Fig. 5c) suggests that above a certain $\delta^{18}\text{O}_{\text{water}}$ threshold, aquatic
606 370 productivity begins to decline. The interpretation of $\delta^{13}\text{C}_{\text{ostracod}}$ in some coastal lakes, may
607 371 therefore be dependent on understanding of the range of expected $\delta^{18}\text{O}_{\text{water}}$. Where there is a
608 372 shift to a positive relationship between $\delta^{18}\text{O}_{\text{ostracod}}$ and $\delta^{13}\text{C}_{\text{ostracod}}$, it reflects a major change in
609 373 hydrological budget (Schwalb, 2003) for example precipitation to seawater as the primary
610 374 hydrological input. If this relationship is therefore seen in palaeo-dataset, it may be used to
611 375 identify changes in freshwater/seawater input to coastal lakes. Although generally accepted
612 376 that coastal lagoons, lakes, and ponds have relatively little freshwater input (Oertel, 2005), it
613 377 is possible that some coastal lakes may have very large variations in salinity and at times have
614 378 very low salinity as a result of large inputs of meteoric water. In estuaries, increased freshwater
615 379 inputs from increased river discharge are known to increase primarily productivity (Underwood
616 380 and Kromkamp, 1999) due to increased nutrient loading. It is possible, therefore, that in
617 381 Pegwell Bay increased precipitation is driving nutrient loading from surface run-off of the
618 382 surrounding salt marsh, and thus increasing productivity. Conversely, during times of
619 383 increased seawater input, tidal cycles and direct oceanic connection are increasing turbidity
620 384 and thus decreasing aquatic productivity.
621 385
622 386

631 387 $\delta^{18}\text{O}_{\text{water}}$ values in coastal lakes may therefore represent variations in inputs of meteoric water
632 388 and seawater, suggesting that $\delta^{18}\text{O}_{\text{ostracod}}$ is related to importance of inputs into the
633 389 hydrological budget. Samples that show a relationship with temperature, as defined by Kim
634 390 and O'Neil (1997), are those shells with higher $\delta^{18}\text{O}$ while shells with lower $\delta^{18}\text{O}$ do not follow
635 391 a thermodynamic relationship (Fig. 5a), suggesting $\delta^{18}\text{O}_{\text{water}}$, and hydrological budget, as a
636 392 more important control than temperature. If bulk multiple shells are analysed (i.e. many shells
637 393 combined together as one sample) that contains individuals from multiple generations, which
638 394 may not all relate to temperature, it is likely that temperatures cannot be accurately
639 395 reconstructed. Where multiple single individuals are analysed, the spread of $\text{Mg}/\text{Ca}_{\text{ostracod}}$
640 396 values used alongside the range of $\delta^{18}\text{O}_{\text{ostracod}}$ may aid in identifying where a temperature
641 397 signal is present.
642 398

643 399 **5. Conclusions**

650 400
651 401 The study highlights the importance of modern systematic studies, particularly in highly
652 402 complex and variable environments such as coastal lakes. However, even with good
653 403 understanding of modern environments, the interpretation of palaeo-stable isotope datasets
654 404 for *C. torosa* is complex. In most circumstances, $\delta^{18}\text{O}_{\text{water}}$ is a more dominant control on
655
656
657
658
659
660

661
662
663 405 $\delta^{18}\text{O}_{\text{ostracod}}$, but with a dependence on temperature when there is a direct marine influence and
664
665 406 high $\delta^{18}\text{O}_{\text{water}}$. Since there is a shift in relationship between $\delta^{18}\text{O}_{\text{ostracod}}$ and $\delta^{13}\text{C}_{\text{ostracod}}$ between
666 407 the populations that follow the water temperature/ $\delta^{18}\text{O}_{\text{ostracod}}$ relationship and those that do
667
668 408 not, if multiple individuals per stratigraphic level are analysed and the resulting $\delta^{18}\text{O}_{\text{ostracod}}$ and
669 409 $\delta^{13}\text{C}_{\text{ostracod}}$ data combined, it may be possible to determine if the direction of change indicates
670
671 410 a population that can be used as a proxy for temperature. It is clear, therefore, that simplistic
672 411 interpretations of $\delta^{18}\text{O}_{\text{ostracod}}$ data with or without modern data may be misleading. We
673
674 412 recommend that for future palaeoenvironmental research in marginal marine environments,
675 413 stable isotope analyses should be: 1) undertaken on multiple single shells; and 2) where
676 414 carapaces are preserved, paired with trace-element/Ca analyses on the same individual.
677
678 415

679 416 **Acknowledgements**

680
681 417
682 418 The research was funded by a studentship from the UK Natural Environment Research
683
684 419 Council as part of the London NERC DTP (NE/L002485/1). The authors thank Miles Irving for
685 420 cartography assistance with Figure 1. We are grateful to John McAllister (Head of Reserves
686
687 421 (East), Kent Wildlife Trust) for permission to monitor water temperatures and collect samples
688 422 in the Pegwell Bay pond.
689
690 423

691 424 **References**

- 692 425
693 426 Anadón, P., F. Burjachs, M. Martín, J. Rodríguez-Lazaro, F. Robles, R. Utrilla & A. Vazquez, 2002.
694 427 Paleoenvironmental evolution of the Pliocene Villarroya Lake, northern Spain. A
695 428 multidisciplinary approach. *Sedimentary Geology* 148(1-2):9-27.
696 429 Anadón, P., A. Moscariello, J. Rodríguez-Lazaro & M. L. Filippi, 2006. Holocene environmental
697 430 changes of Lake Geneva (Lac Lemán) from stable isotopes ($\delta^{13}\text{C}$, $\delta^{18}\text{O}$) and
698 431 trace element records of ostracod and gastropod carbonates. *Journal of Paleolimnology*
699 432 35(3):593-616.
700 433 Bodergat, A. M., C. Lecuyer, F. Martineau, A. Nazik, K. Gurbuz & S. Legendre, 2014. Oxygen
701 434 isotope variability in calcite shells of the ostracod *Cyprideis torosa* in Akyatan Lagoon,
702 435 Turkey. *Journal of Paleolimnology* 52(1-2):43-59.
703 436 Bridgwater, N. D., T. H. E. Heaton & S. L. O'Hara, 1999. A late Holocene palaeolimnological record
704 437 from central Mexico, based on faunal and stable-isotope analysis of ostracod shells. *Journal*
705 438 *of Paleolimnology* 22(4):383-397.
706 439 Carbonel, P., 1988. Ostracods and the transition between fresh and saline waters. In P. De
707 440 Deckker, J.-P. Colin & J.-P. Peypouquet (Eds.) *Ostracoda in the earth sciences*: 157-173.
708 441 Amsterdam: Elsevier.
709 442 Chester, R., 2000. Marine geochemistry, 1 edn. John Wiley & Sons.
710 443 Chivas, A. R., P. De Deckker, S. X. Wang & J. A. Cali, 2002. Oxygen-isotope systematics of the
711 444 nektic ostracod *Australocypris robusta*. In Holmes, J. A. & A. R. Chivas (Eds) *The*
712 445 *Ostracoda: Applications in Quaternary Research*. American Geophysical Union, Geophysical
713 446 Monograph, 13: 301-313. Washington D.C.: AGU.
714 447 Coplen, T. B., C. Kendall & J. Hopple, 1983. Comparison of Stable Isotope Reference Samples.
715 448 *Nature* 302(5905):236-238.

721
722
723
724
725
726
727
728
729
730
731
732
733
734
735
736
737
738
739
740
741
742
743
744
745
746
747
748
749
750
751
752
753
754
755
756
757
758
759
760
761
762
763
764
765
766
767
768
769
770
771
772
773
774
775
776
777
778
779
780

449 Darling, W.G., Talbot, J.C., 2003. The O & H stable isotopic composition of fresh waters in the
450 British Isles. 1. Rainfall. *Hydrology and Earth System Sciences* 7, 163-181.

451 De Deckker, P., A. R. Chivas & J. M. G. Shelley, 1999. Uptake of Mg and Sr in the euryhaline
452 ostracod *Cyprideis* determined from in vitro experiments. *Palaeogeography,*
453 *Palaeoclimatology, Palaeoecology* 148(1-3):105-116.

454 De Deckker, P. & A. Lord, 2017. *Cyprideis torosa*: a model organism for the Ostracoda? *Journal of*
455 *Micropalaeontology* 36(1), 3-6

456 Decrouy, L., T. W. Vennemann & D. Ariztegui, 2011. Controls on ostracod valve geochemistry: Part
457 2. Carbon and oxygen isotope compositions. *Geochimica Et Cosmochimica Acta*
458 75(22):7380-7399.

459 Dettman, D. L., A. J. Smith, D. K. Rea, T. C. Moore & K. C. Lohmann, 1995. Glacial meltwater in
460 Lake Huron inferred from single-valve analysis of oxygen isotopes in ostracodes. *Quaternary*
461 *Research* 43:297-310.

462 Dix, G. R., R. T. Patterson & L. E. Park, 1999. Marine saline ponds as sedimentary archives of late
463 Holocene climate and sea-level variation along a carbonate platform margin: Lee Stocking
464 Island, Bahamas. *Palaeogeography, Palaeoclimatology, Palaeoecology* 150(3-4):223-246.

465 Google Maps Street View. 'Sandwich Road Street View' [Map], Google,
466 <https://goo.gl/maps/LMVmosyEEqN2>; accessed 07-Apr-20.

467 Heaton, T. H. E., J. A. Holmes & N. D. Bridgwater, 1995. Carbon and oxygen isotope variations
468 among lacustrine ostracods: Implications for palaeoclimatic studies. *Holocene* 5(4):428-434.

469 Heip, C., 1976. The life-cycle of *Cyprideis torosa* (Crustacea, Ostracoda). *Oecologia* 24(3):229-245.

470 Hodell, D. A., J. H. Curtis, G. A. Jones, A. Higuera-Gundy, M. Brenner, M. W. Binford & K. T. Dorsey,
471 1991. Reconstruction of Caribbean climate change over the past 10,500 years. *Nature*
472 352(6338):790-793.

473 Holmes, J. A., T. Atkinson, D. P. F. Darbyshire, D. J. Horne, J. Joordens, M. B. Roberts, K. J. Sinka
474 & J. E. Whittaker, 2010. Middle Pleistocene climate and hydrological environment at the
475 Boxgrove hominin site (West Sussex, UK) from ostracod records. *Quaternary Science*
476 *Reviews* 29(13-14):1515-1527

477 Ingram, B. L., P. De Deckker, A. R. Chivas, M. E. Conrad & A. R. Byrne, 1998. Stable isotopes,
478 Sr/Ca, and Mg/Ca in biogenic carbonates from Petaluma Marsh, northern California, USA.
479 *Geochimica Et Cosmochimica Acta* 62(19-20):3229-3237.

480 Janz, H. & T. W. Vennemann, 2005. Isotopic composition (O, C, Sr, and Nd) and trace element
481 ratios (Sr/Ca, Mg/Ca) of Miocene marine and brackish ostracods from North Alpine Foreland
482 deposits (Germany and Austria) as indicators for palaeoclimate. *Palaeogeography,*
483 *Palaeoclimatology, Palaeoecology* 225(1-4):216-247.

484 Keatings, K. W., T. H. E. Heaton & J. A. Holmes, 2002. Carbon and oxygen isotope fractionation in
485 non-marine ostracods: Results from a 'natural culture' environment. *Geochimica Et*
486 *Cosmochimica Acta* 66(10):1701-1711.

487 Keatings, K., I. Hawkes, J. Holmes, R. Flower, M. Leng, R. Abu-Zied & A. Lord, 2007. Evaluation of
488 ostracod-based palaeoenvironmental reconstruction with instrumental data from the arid
489 Faiyum Depression, Egypt. *Journal of Paleolimnology* 38(2):261-283.

490 Kim, S. T. & J. R. Oneil, 1997. Equilibrium and nonequilibrium oxygen isotope effects in synthetic
491 carbonates. *Geochimica Et Cosmochimica Acta* 61(16):3461-3475.

492 Leng, M. J. & J. D. Marshall, 2004. Palaeoclimate interpretation of stable isotope data from lake
493 sediment archives. *Quaternary Science Reviews* 23(7-8):811-831.

494 Li, X. & W. Liu, 2014. Water salinity and productivity recorded by ostracod assemblages and their
495 carbon isotopes since the early Holocene at Lake Qinghai on the northeastern Qinghai–
496 Tibet Plateau, China. *Palaeogeography, Palaeoclimatology, Palaeoecology* 407:25-33.

497 Marco-Barba, J., E. Ito, E. Carbonell & F. Mesquita-Joanes, 2012. Empirical calibration of shell
498 chemistry of *Cyprideis torosa* (Jones, 1850) (Crustacea: Ostracoda). *Geochimica Et*
499 *Cosmochimica Acta* 93:143-163.

500 Met Office (2012): Met Office Integrated Data Archive System (MIDAS) Land and Marine Surface
501 Stations Data (1853-current). NCAS British Atmospheric Data
502 Centre, 2017. <http://catalogue.ceda.ac.uk/uuid/220a65615218d5c9cc9e4785a3234bd0>

781
782
783
784
785
786
787
788
789
790
791
792
793
794
795
796
797
798
799
800
801
802
803
804
805
806
807
808
809
810
811
812
813
814
815
816
817
818
819
820
821
822
823
824
825
826
827
828
829
830
831
832
833
834
835
836
837
838
839
840

Oertel, G. F., 2005. Coastal Lakes and Lagoons. In Schwartz, M. L. (ed) *Encyclopedia of Coastal Science*. Springer Netherlands, Dordrecht, 263-266.

Pint, A. & P. Frenzel, 2017. Ostracod fauna associated with *Cyprideis torosa* - An overview. *Journal of Micropalaeontology* 36(1):113-119.

Roberts, L. R., J. A. Holmes & D. J. Horne, 2020. Tracking the seasonal calcification of *Cyprideis torosa* (Crustacea, Ostracoda) using Mg/Ca-inferred temperatures, and its implications for palaeotemperature reconstruction. *Marine Micropaleontology* 156:101838.

Romanek, C. S., E. L. Grossman & J. W. Morse, 1992. Carbon Isotopic Fractionation in Synthetic Aragonite and Calcite - Effects of Temperature and Precipitation Rate. *Geochimica Et Cosmochimica Acta* 56(1):419-430.

Scharf, B., M. Herzog & A. Pint, 2017. New occurrences of *Cyprideis torosa* (Crustacea, Ostracoda) in Germany. *Journal of Micropalaeontology* 36(1):120-126

Schwalb, A., 2003. Lacustrine ostracodes as stable isotope recorders of late-glacial and Holocene environmental dynamics and climate. *Journal of Paleolimnology* 29(3):267-351.

Street-Perrott, F. A., J. A. Holmes, M. P. Waller, M. J. Allen, N. G. H. Barber, P. A. Fothergill, D. D. Harkness, M. Ivanovich, D. Kroon & R. A. Perrott, 2000. Drought and dust deposition in the West African Sahel: A 5500-year record from Kajemarum Oasis, northeastern Nigeria. *Holocene* 10(3):293-302.

Underwood, G. J. C. & J. Kromkamp, 1999. Primary Production by Phytoplankton and Microphytobenthos in Estuaries. In Nedwell, D. B. & D. G. Raffaelli (Eds) *Advances in Ecological Research*. 29: 93-153. Amsterdam: Academic Press.

von Grafenstein, U., 2002. Oxygen-isotope studies of ostracods from deep lakes. In Holmes, J. A. & A. R. Chivas (Eds) *The Ostracoda: Applications in Quaternary Research*. American Geophysical Union, Geophysical Monograph, 13: 249-266. Washington D.C.: AGU.

von Grafenstein, U., H. Erlenkeuser & P. Trimborn, 1999a. Oxygen and carbon isotopes in modern fresh-water ostracod valves: assessing vital offsets and autecological effects of interest for palaeoclimate studies. *Palaeogeography, Palaeoclimatology, Palaeoecology* 148(1-3):133-152.

von Grafenstein, U., H. Erlenkeuser, A. Brauer, J. Jouzel & S. J. Johnsen, 1999b. A mid-European decadal isotope-climate record from 15,500 to 5000 years BP. *Science* 284(5420):1654-1657.

Wansard, G., 1996. Quantification of paleotemperature changes during isotopic stage 2 in the La Draga continental sequence (NE Spain) based on the Mg/Ca ratio of freshwater ostracods. *Quaternary Science Reviews* 15:237-245.

Williams, M., M. J. Leng, M. H. Stephenson, J. E. Andrews, I. P. Wilkinson, D. J. Siveter, D. J. Horne & J. M. Vannier, 2006. Evidence that Early Carboniferous ostracods colonised coastal flood plain brackish water environments. *Palaeogeography, Palaeoclimatology, Palaeoecology* 230(3-4):299-318.

Wouters, K., 2017. On the modern distribution of the euryhaline species *Cyprideis torosa* (Jones, 1850) (Crustacea, Ostracoda). *Journal of Micropalaeontology* 36(1):21-30

Wrozyna, C., Frenzel, P., Daut, G., Mäusbacher, R., Zhu, L., & Schwalb, A. (2012). Holocene lake-level changes of Lake Nam Co, Tibetan Plateau, deduced from ostracod assemblages and $\delta^{18}\text{O}$ and $\delta^{13}\text{C}$ signatures of their valves. In D.J. Horne, J. Holmes, J. Rodriguez-Lazaro & F.A. Viehberg (Eds.), *Ostracoda as proxies for Quaternary climate* (Vol. 17, pp. 281-295). Amsterdam: Elsevier

Xia, J., B. J. Haskell, D. R. Engstrom & E. Ito, 1997. Holocene climate reconstructions from tandem trace-element and stable-isotope composition of ostracodes from Coldwater Lake, North Dakota, USA. *Journal of Paleolimnology* 17(1):85-100.

List of Figures

Figure 1. Location of the coastal pond at Pegwell Bay. The black triangle adjacent to Ramsgate harbour denotes the location of the seawater end member water sample taken on

841
842
843 555 18-Apr-2017. The inset map shows the location of samples taken on 27-Jun-2017. Samples
844 556 were collected at 'X' for all sample dates and the triangle .

846 557
847 558 **Figure 2.** a) $\delta^{18}\text{O}_{\text{water}}$, b) electrical conductivity, c) average water temperature, d) $\delta^{18}\text{O}_{\text{ostracod}}$
848 559 e) $\text{Mg}/\text{Ca}_{\text{ostracod}}$, and d) $\delta^{13}\text{C}_{\text{ostracod}}$ for each sampling day. Data from individual valves are
850 560 represented by the grey circles and the mean is denoted by the black line

852 561
853 562 **Figure 3.** Relationship between $\delta^{18}\text{O}_{\text{water}}$ and electrical conductivity over the sampling year.
854 563 The triangle denotes the seawater end member sampled adjacent to Ramsgate Harbour on
855 564 18-Apr-17.

857 565
858 566 **Figure 4.** $\delta^2\text{H}$ and $\delta^{18}\text{O}$ values for water sampled in April and June from the coastal pond. The
859 567 triangle denotes the seawater end member sampled adjacent to Ramsgate Harbour on 18-
860 568 Apr-17. The solid black line denotes the Global Meteoric Water Line (GMWL). The dashed
861 569 line denotes the local evaporation line (LEL) of $y = 4.1x - 4.3$ (R^2 0.97).

864 570
865 571 **Figure 5.** Relationships between a) $\delta^{18}\text{O}_{\text{ostracod}}$ and Mg/Ca -inferred temperature b) $\delta^{18}\text{O}_{\text{ostracod}}$
866 572 and $\text{Sr}/\text{Ca}_{\text{ostracod}}$, c) $\delta^{18}\text{O}_{\text{ostracod}}$ and $\delta^{13}\text{C}_{\text{ostracod}}$ and d) $\text{Mg}/\text{Ca}_{\text{ostracod}}$ and $\text{Sr}/\text{Ca}_{\text{ostracod}}$. The purple
867 573 line in (a) shows the relationship between water temperature and calcite oxygen-isotope
868 574 value based on the equation of Kim and O'Neil (1997)

871 575
872 576
873 576 **Figure 6.** PCA biplots of environmental variables for each sampling day

874 577 875 578 **List of Tables**

876 579
877 580 **Table 1.** Electrical conductivity, average water temperature, $\delta^{18}\text{O}$, and $\delta^2\text{H}$ for each of the
878 581 sampling days. Temperature is the average recorded over a 24-hour period, except for 4-Aug-
880 582 18, which is averaged from data logger deployment at 14:40.

881 583
882 584
883 584 **Table 2.** Water chemistry variables recorded from high to low tide on 27-Jun-17. Numbers
884 585 appearing after the 12:00 sampling times (1,2 etc.) relate to the locations in Figure 1.

885 586
886 587
887 587 **Table 3.** Ostracod Mg/Ca , $\delta^{18}\text{O}$ and $\delta^{13}\text{C}$ for individual carapaces collected on each
888 588 sampling day. The trace element/ Ca and isotope analyses are from the same carapace.

889 589
890 590
891 590 **Table 4.** Minimum, maximum and average monthly air and water temperature, and monthly
892 591 rainfall for the monitoring period August 2016 to September 2017. Air temperature and
893 592 precipitation data were downloaded from Met Office (2012)

901
902
903 593
904 594 **Table 1.** Electrical conductivity, average water temperature, $\delta^{18}\text{O}$, and $\delta^2\text{OH}$ for each of the
905
906 595 sampling days. Temperature is the average recorded over a 24-hour period, except for 4-Aug-
907 596 18, which is averaged from data logger deployment at 14:40.
908
909 597
910 598

Date	Electrical conductivity (mS cm ⁻¹)	Salinity PSU	Average water temperature (°C)	$\delta^{18}\text{O}$ (‰ VSMOW)	$\delta^2\text{H}$ (‰ VSMOW)
04-Aug-16	55.2	36.6	20.9	+3.86	
01-Dec-16	40.2	25.7	3.0	-2.84	
02-Feb-17	45.1	29.2	8.3	-1.46	
18-Apr-17	44.6	28.8	10.2	-1.19	+1.3
27-Jun-17	75.2	~53*	17.2	+4.85	+15.48
28-Sep-17	33.3	20.8	18.3	-0.06	-6.3
Ramsgate				+0.27	+1.6

919
920 599 *above scale for accurate conversion
921

922 600
923 601 **Table 2.** Water chemistry variables recorded from high to low tide on 27-Jun-17. Numbers
924 602 appearing after the 12:00 sampling times (1,2 etc.) relate to the locations in Figure 1.
925
926 603
927 604

Time / Location	$\delta^{18}\text{O}$ (‰)	$\delta^2\text{H}$ (‰)	Electrical conductivity (mS cm ⁻¹)	Water Temp. (°C)	Alkalinity as CaCO ₃ equivalence (mg L ⁻¹)	
					CO ₃ ²⁻	HCO ₃ ⁻
06:00	+5.28	+16.7	70.5	15.8	0	266
07:00	+5.20	+16.8	75.0	16.4	0	266
08:00	+5.18	+16.2	75.9	17.6	0	244
08:30	+4.28	+10.6				
09:00	+5.14	+16.5	77.8	19.0	0	256
10:00	+5.11	+16.2	76.9	19.4	0	272
12:00-1	+5.17	+15.0	77.8	22.5	0	270
12:00-2	+4.92	+17.4	76.7	21.6		
12:00-3	+4.29	+16.2	72.3	21.5		
12:00-4	+4.06	+16.2	70.2	23.2		
12:00-5	+4.14	+12.9	71.7	21.9		
12:00-6	+4.24	+14.8	71.9	22.2		
14:00	+5.09	+16.3	77.9	23.3	0	260
15:00	+5.07	+17.8	78.2	24.7	14	254
17:00	+5.11	+17.3	78.8	22.6	0	248
Average	+4.82	+15.4	75.2	20.8		
Std Dev.	±0.46	±2.03	±3.0	±2.7		

949 605
950 606
951 607 **Table 3.** Ostracod Mg/Ca, Mg/Ca-inferred temperature, $\delta^{18}\text{O}_{\text{shell}}$, back-calculated $\delta^{18}\text{O}_{\text{water}}$,
952 608 and $\delta^{13}\text{C}_{\text{shell}}$ for individual carapaces collected on each sampling day. The trace element/Ca
953 609 and isotope analyses are from the same carapace.
954 609
955
956 610
957
958
959
960

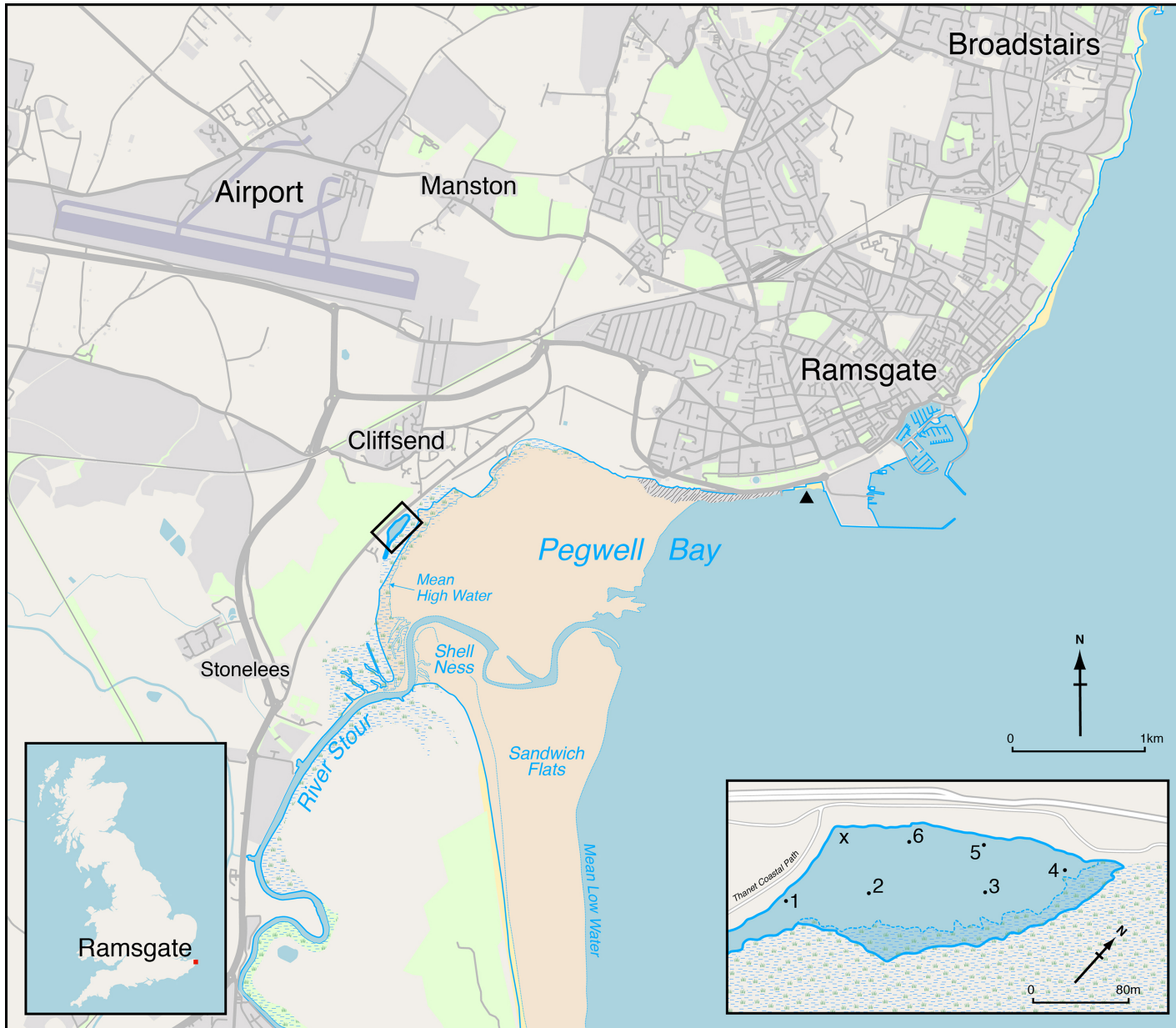
961
962
963
964
965
966
967
968
969
970
971
972
973
974
975
976
977
978
979
980
981
982
983
984
985
986
987
988
989
990
991
992
993
994
995
996
997
998
999
1000
1001
1002
1003
1004
1005
1006
1007
1008
1009
1010
1011
1012
1013
1014
1015
1016
1017
1018
1019
1020

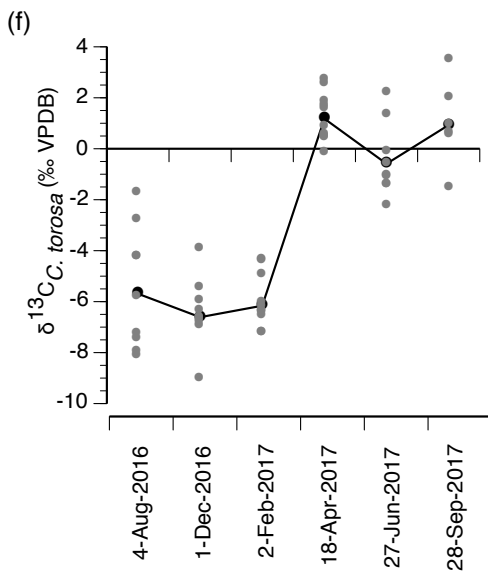
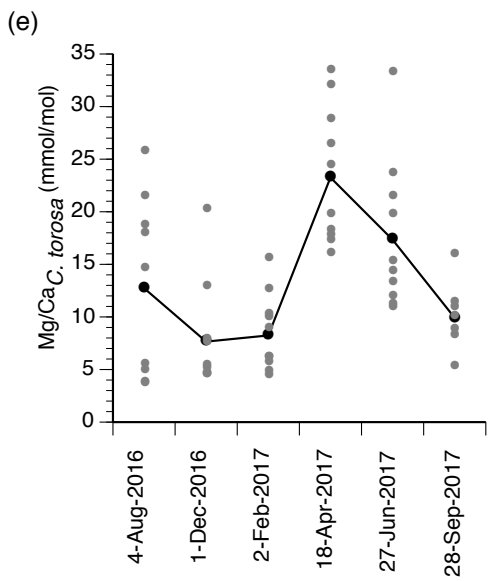
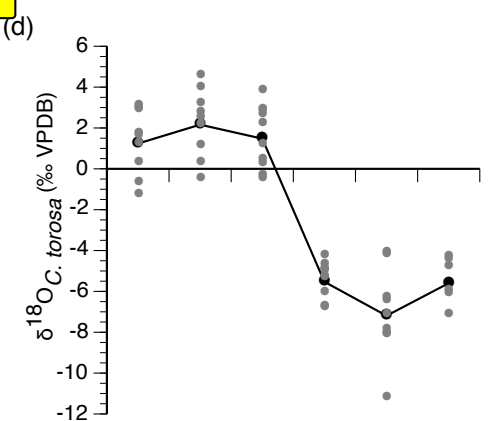
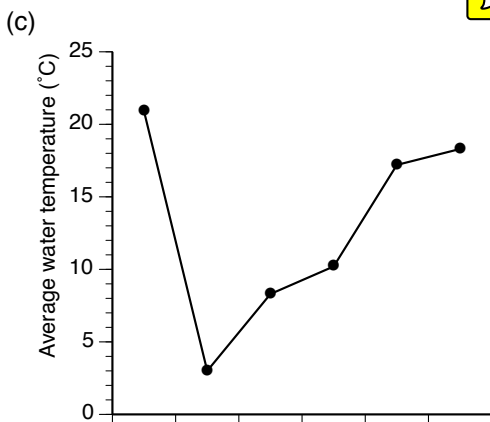
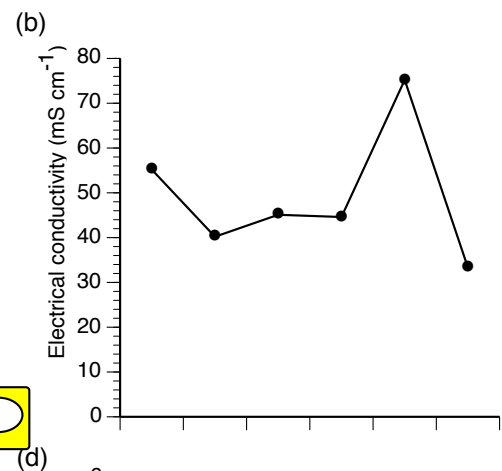
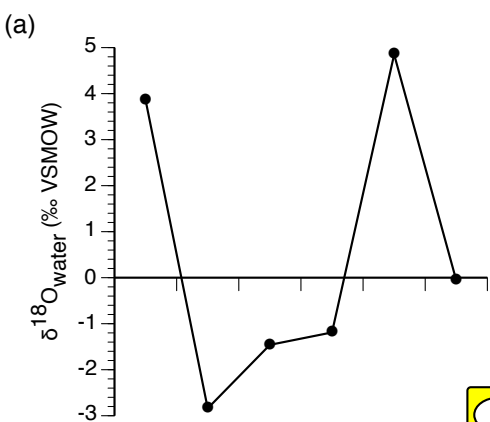
Collected	Mg/Ca _{ostracod} (mmol/mol)	Mg/Ca- inferred Temperature (°C)	δ ¹⁸ O _{ostracod} (‰)	Back- calculate d δ ¹⁸ O _{water} (‰)	δ ¹³ C _{ostracod} (‰)
	18.57	25.8	0.19	2.70	-2.91
	4.68	8.5	2.9	1.72	-7.67
	3.58	7.1	1.56	0.06	-8.35
	5.24	9.2	3.00	1.98	-7.45
04-Aug-16	17.78	24.8	1.65	3.96	-1.84
	14.39	20.6	-0.77	0.68	-6.01
	3.48	7	2.81	1.28	-8.20
	25.57	34.5	1.16	5.37	-4.41
	21.34	29.3	-1.37	1.83	-4.38
	12.75	18.6	2.08	3.11	-6.14
	4.93	8.8	2.44	1.33	-6.82
	7.64	12.2	3.12	2.77	-7.14
	4.35	8.1	4.49	3.22	-9.26
01-Dec-16	4.42	8.2	0.22	-1.03	-5.64
	7.33	11.8	2.69	2.25	-6.88
	4.27	8	-0.57	-1.86	-6.97
	20.05	27.7	1.07	3.95	-4.09
	5.19	9.2	3.92	2.90	-6.56
	4.57	8.4	-0.56	-1.76	-6.58
	4.24	8	-0.41	-1.71	-6.38
	5.48	9.5	0.16	-0.79	-5.13
	5.92	10.1	0.35	-0.47	-4.55
02-Feb-17	15.37	21.8	1.1	2.80	-4.52
	10.03	15.2	2.84	3.14	-7.41
	12.46	18.2	2.14	3.09	-6.58
	9.72	14.8	2.79	3.01	-6.25
	5.94	10.1	3.77	2.95	-6.76
	8.66	13.5	2.59	2.53	-7.42
	17.56	24.6	-5.45	-3.19	1.62
	18.03	25.1	-6.20	-3.83	-0.25
	28.67	38.4	-6.89	-1.95	2.64
	15.87	22.5	-5.10	-3.26	1.51
18-Apr-17	17.1	24	-5.41	-3.26	1.78
	24.24	32.9	-6.93	-3.03	2.48
	19.61	27.1	-5.08	-2.31	0.8
	33.32	44.2	-4.79	1.22	0.33
	31.91	42.4	-5.06	0.63	0.48
	26.26	35.4	-4.38	0.00	0.4

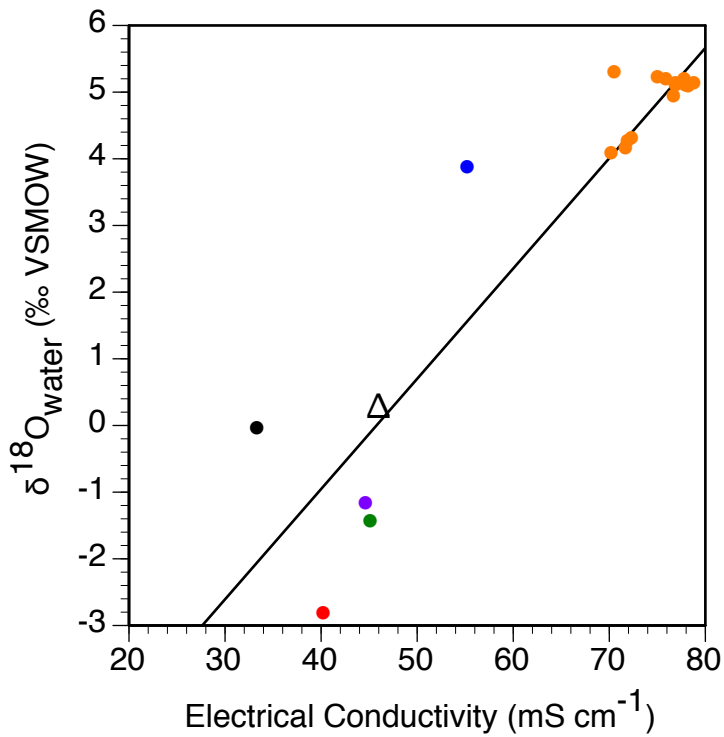
		13.06	19	-8.23	-7.12	-0.71
		33.12	43.9	-6.44	-0.49	-0.20
		21.34	29.3	-4.31	-1.10	2.14
		11.8	17.4	-4.21	-3.44	1.27
	27-Jun-17	23.5	32	-11.38	-7.65	-2.37
		15.11	21.5	-6.61	-4.97	-1.15
		11.01	27.1	-8.26	-5.49	-1.19
		14.18	16.4	-8.03	-7.47	-1.52
		10.67	20.3	-7.26	-5.88	-1.54
		9.89	16	-4.42	-3.95	0.87
		8.07	15	-4.93	-4.67	1.95
	28-Sep-17	5.08	12.7	-6.26	-6.50	0.45
		8.63	9	-4.59	-5.66	0.53
		11.22	13.4	-6.11	-6.20	3.44
		15.77	16.7	-7.28	-6.65	-1.66

Table 4. Minimum, maximum and average monthly air and water temperature, and monthly rainfall for the monitoring period August 2016 to September 2017. Air temperature and precipitation data were downloaded from Met Office (2012)

Month/Year	Air temp. (°C)			Water temp. (°C)			Precipitation (mm)
	Max.	Min.	Average	Max.	Min.	Average	
08/2016	23.3	14.4	18.5	27.4	13.0	19.4	18.0
09/2016	22.5	14.4	17.7	26.6	14.7	19.6	76.2
10/2016	15.0	9.4	11.9	17.1	9.8	12.8	34.8
11/2016	10.1	4.4	7.4	12.6	2.1	7.8	103.4
12/2016	9.3	3.8	6.8	10.1	0.4	5.7	9.2
01/2017	6.3	0.7	3.5	7.7	-1.6	3.3	48.2
02/2017	9.2	4.5	6.6	11.3	1.2	6.4	26.4
03/2017	13.0	6.0	9.2	16.4	4.7	10.2	17.2
04/2017	13.7	5.9	9.4	21.6	5.5	13.9	10.8
05/2017	17.9	9.9	13.5	31.0	8.1	17.6	57.8
06/2017	22.4	13.1	17.4	34.2	11.8	21.4	37.8
07/2017	22.8	14.5	18.0	30.9	13.9	20.6	74.2
08/2017	21.4	13.3	16.9	25.9	15.6	20.2	85.6
09/2017	18.3	11.1	14.3	22.9	12.3	16.8	37.0







● 4-Aug-2016

● 18-Apr-2017

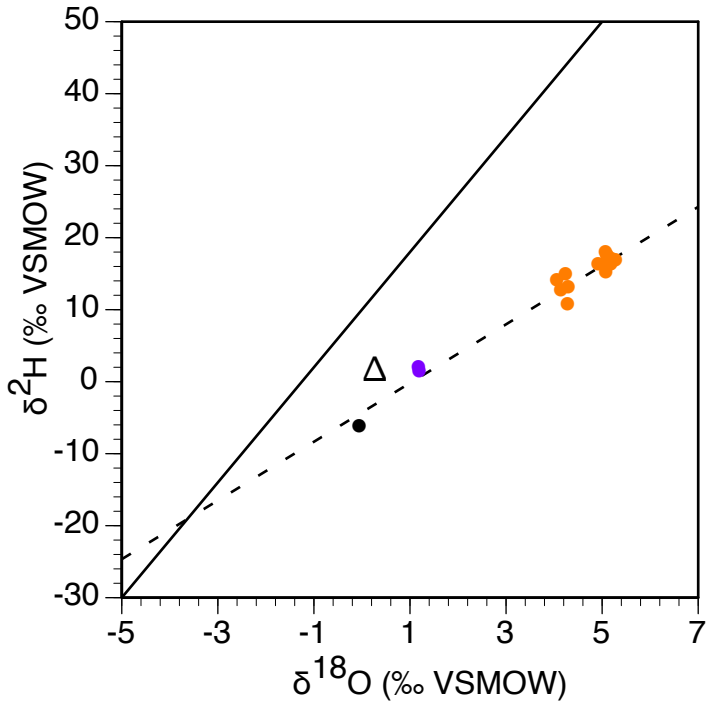
● 1-Dec-2016

● 27-Jun-2017

△ Ramsgate Harbour seawater

● 2-Feb-2017

● 28-Sep-2017



● 18-Apr-2017

● 28-Sep-2017

● 27-Jun-2017

△ Ramsgate Harbour seawater

